

SOME FEATURES OF POLARIZED LIDAR SENSING OF THE ATMOSPHERE-OCEAN SYSTEM

G.M. Krekov, M.M. Krekova

Institute of Atmospheric Optics, Tomsk, 634055

Received August 1, 1988

The paper presents Monte Carlo calculations of the polarization parameters of lidar returns from the sea. We study their dependence on such optical characteristics of the medium as the scattering phase function, extinction coefficient, and absorption coefficient, as well as on the experimental geometry. Estimates are made for $\lambda = 0.5 \mu\text{m}$, with the scattering matrices close in the form to the Rayleigh matrix. The air-water interface is assumed to be a plane-stratified surface.

Recent work involving the use of laser sensing techniques to development. On the one hand, lidar methods are quite promising as diagnostics of the upper oceanic layer; on the other, there exist many difficulties in the inversion of lidar data due to the influence of the atmosphere and the interface between the two media. Success in interpreting of the data obtained for the propagation of short laser pulses into the ocean strongly depends upon a correct analysis of a variety of measurement techniques and numerical simulations.

In this paper, we attempt to study the use of polarized radiation for sensing naturally occurring bodies of water. It should be noted that only a few relevant papers, either theoretical or experimental, are to be found in the literature. The lack of theoretical studies of this problem is due not only to the complexity of the mathematical apparatus, but also to the lack of a sufficiently large volume of data on the scattering matrices of sea water. At the same time, the available data for the scattering matrix are contradictory with regard to the form of the matrix itself.

In the present paper, we present data on the polarization characteristics of the return signal obtained by numerical simulation of ocean sensing, with a hypothetical lidar system aboard an aircraft.

An objective theoretical analysis can be based on the solution of the nonstationary vector equation of radiative transfer. It is reasonable, taking into account the variety of the composition of sea water, to assume that the scattering properties can be described by a scattering matrix in which the number of nonzero elements depends on the nature of the particles. Starting with this fact, one should seek a method to solve the vector radiative transfer equation which uses the general form of the scattering matrix. These requirements can be satisfied by a numerical statistical method, enabling one to construct a solution algorithm which uses the scattering matrix in a general form, and provides for separation of interactions of different multiplicity. Omitting a detailed description and justification for this algorithm^{1,2}, we note only the main features of the problem. Its initial and boundary conditions correspond

to a typical single ended scheme of laser sensing². It is assumed that a linearly polarized optical pulse described by a δ -function in time is normally incident upon a plane-parallel scattering layer. The light source is assumed to be a circle in the plane $Y = 0$ in a system of spatial coordinates $r(\bar{x}, y, z)$ and angular coordinates $\Omega(a, b, c)$, where it emits isotropically into a cone of directions $\cos\phi_s \leq b \leq 1$. The receiver is also defined as a circle with a number of angular fields of view $\cos\phi_r^i \leq b \leq 1$, $i = 1, 2, \dots$. The lidar system is in the atmosphere at the height H_0 above the sea surface (which has no waves). The optical properties of the atmosphere above the surface are defined in accordance with models of the coarse component of the sea haze of the boundary atmospheric layer described in Ref. 3 for "dry" and "humid" atmospheres. The dry-atmosphere model assumes that aerosol particles are crystals of NaCl, whose scattering matrix was based on the data presented in Ref. 4. The scattering matrix for the humid-atmosphere model was calculated using the Mie formulas. The initial state of the polarization vector was given the form $\bar{F}(I, Q, U, V) = \bar{F}^0(I, Q, U, V)$. We are interested in finding the polarization characteristics of the lidar return $F(I, Q, U, V)$ as a function of optical state of the and the geometry of the receiver. Construction of the algorithm used a modification of the local-estimate method which takes into account the marked asymmetry of the scattering phase function of sea water⁵. It was also taken into account in the course of solving the problem that there exist several mechanisms of extinction in sea water, namely, scattering and absorption of light by the water itself, and also by suspended particles, with absorption by the latter being mainly due to chlorophyll in phytoplankton and dissolved organics (yellow matter).

Accordingly, the total extinction coefficient σ_{ext} is

$$\sigma_{\text{ext}} = \sigma_{\text{sw}} + \sigma_{\text{aw}} + \sigma_{\text{sh}} + C_{\text{ch}} K_{\text{ch}} + C_{\text{ym}} K_{\text{ym}},$$

where σ_s and σ_a are the coefficients of extinction due to scattering and absorption by water and hydrosol, C_{ch} ,

C_{ys} and κ_{ch} , κ_{ys} are the concentrations and absorptivity of chlorophyll and yellow matter, respectively.

We now describe the selection of scattering matrices for hydrosols in more detail. For this purpose we used data sets obtained from measurements in different regions of the Pacific and Atlantic Oceans⁶, in the Baltic Sea⁹, and in model media^{7,8}. Scattering matrices in these references have the form

$$\hat{S} = \begin{vmatrix} S_{11} & S_{12} & 0 & 0 \\ S_{21} & S_{22} & 0 & 0 \\ 0 & 0 & S_{33} & S_{34} \\ 0 & 0 & S_{43} & S_{44} \end{vmatrix}$$

Elements S_{43} and S_{34} of the matrix are close to zero, and $S_{12} = S_{21}$. As follows from other series of measurements^{10,11} all elements of the scattering matrices differ from zero (except S_{31} and S_{42}) and are independent of each other. The use of such matrices in calculations is practically impossible because of the fact that the asymmetry of the matrix elements can either indicate the existence of particle orientation or optical activity. In either case, the data in these papers do not admit of a full characterization of the radiative properties of an elementary volume, since there is no information about the azimuthal distribution of scattered radiation, to say nothing of the elements of the extinction matrix.

Most of the calculations made use of the scattering matrices presented in Ref. 6. Those matrices are composed of averaged tabular data comprising more than 200 measurements made in different regions of the Pacific and Atlantic Oceans. The variance of the measurements of elements of \hat{S} is approximately 10% for different water samples. At the same time, there is a significant difference between the scattering phase functions of water from the Pacific and Atlantic Oceans, especially at scattering angles smaller than 30° and larger than 120°. In Ref. 6, these scattering functions were given only graphically. Since these data could not provide us with sufficient numerical accuracy, we recalculated the scattering phase functions using the Mie formulas and size spectra in the form of superposition of power-law spectra $f_i(r) = \sum_i a_i r^{-\nu_i}$, as suggested in

Ref. 12. The parameters of the spectra were varied so that the final numerical results reproduced the qualitative features of the experimentally measured scattering phase functions. It should be noted that hydrosol suspensions involve particles of mineral and organic origin whose indices of refraction are $n = 1.15 - 0.0001i$ and $n = 1.03 - 0.001i$, respectively. As a result, we used the following parameters in calculating of the model scattering phase $g_i(\theta)$ function for waters from the Pacific Ocean:

$$f_i(r) = a_i r^{-\nu_i},$$

where

$$\nu = \begin{cases} 0 & r < 0.01 \mu\text{m} \\ 2.65, & 0.01 \leq r \leq 0.05 \mu\text{m} \\ 3.5, & 0.05 < r \leq 0.1 \mu\text{m} \\ 4.5, & 0.1 < r \leq 1.3 \mu\text{m} \\ 3, & r > 1.3 \mu\text{m} \end{cases}$$

It is assumed that particles with $r > 1.3 \mu\text{m}$ are of organic origin.

For the case of Atlantic waters, the scattering phase function $g_2(\theta)$ has been calculated using the following parameters:

$$f_2(r) = a_2 r^{-\nu},$$

where

$$\nu = \begin{cases} 0., & r \leq 0.01 \mu\text{m} \\ 2.65, & 0.01 \leq r \leq 0.05 \mu\text{m} \\ 4, & 0.05 \leq r < 1.5 \mu\text{m} \\ 3.5, & r \geq 1.5 \mu\text{m} \end{cases}$$

Again, large particles with $r \geq 1.5 \mu\text{m}$ are assumed to be organic. Scattering phase function has stronger asymmetry and enhanced backscattering. Other optical characteristics were taken from Ref. 13:

$$\kappa_{ch} = 0.025 \text{ m}^2/\text{mg}, \kappa_{ym} = 0.022 \text{ m}^2/\text{mg}, \sigma_{aw} = 0.0271 \text{ m}^{-1}, \sigma_{sw} = 0.0023 \text{ m}^{-1}.$$

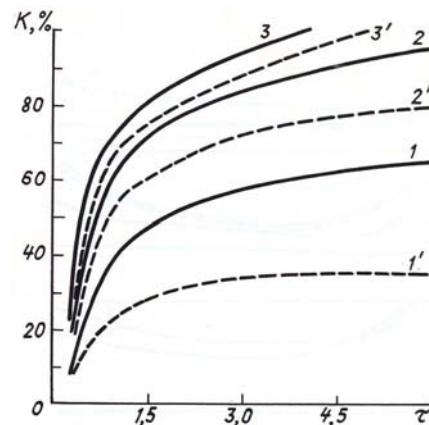


Fig. 1. The ratio $k(\tau) = I_{bg}(\tau)/I(\tau)$ as a function of τ and scattering phase function at $\sigma_{ext} = 0.33 \text{ m}^{-1}$ and $W = 0.835$; $1/2\varphi_s = 0.3 \text{ mrad}$; curves 1 to 3 represent calculations using the scattering phase function $g_1(\theta)$ (curves 1'-3' with $g_2(\theta)$); the value of η was 0.02 for curves 1, 1'; 0.06 for curves 2 and 2'; and 0.12 for curves 3 and 3'.

Let us now consider in more detail the formation of the lidar return signal, prior to the discussion of its polarization properties. Figure 1 presents data illustrating the multiple-scattering contribution of the background to the lidar return, depending on the form of the scattering phase function. The data presented in Fig. 1 were calculated for different values of the parameter $\eta = \varphi_s H_0 \sigma_{ext}/2$, which characterizes the conditions of object illumination. It so happens that at small values of $\eta \leq 0.02$ the lidar return structure

strongly depends on the asymmetry of the scattering phase function. This dependence becomes weaker with increasing of η , and at $\eta > 0.12$, it practically disappears. It should also be noted that the background component is mainly formed at optical depths $\tau \leq 2$ regardless of the η values. Such values of optical depth are normally observed at depth $h \leq 20$ m, since the minimum observed values of σ_{ext} for clear waters are about 0.1 m^{-1} at $\lambda = 0.5 \mu\text{m}$. In practice, the values of σ_{ext} for productive waters exceed 0.3 m^{-1} , and in coastal waters $\sigma_{\text{ext}} \approx 1.5$ to 2 m^{-1} .

Estimates of the influence of the absorbent concentration, the form of scattering phase function and the experimental geometry on the degree of lidar return depolarization are shown in Fig. 2. The calculations were carried out for the "dry" atmosphere model. One outstanding feature of these numerical results is the behavior of the extrema of $\delta(\tau)$ as a function of penetration depth. Such behavior of the depolarization was previously observed in measurements made from aircraft¹⁴. An explanation given in that reference assumed variability of the hydrosol optical properties with depth. As will be shown later, this behavior may be due, to a certain extent, to the influence of the atmospheric ground layer when crystal particles of NaCl are present in it. Residual depolarization of lidar returns in the atmosphere contributes only weakly at narrow angles of the receiver field of view ($\phi_r \leq \phi_s$), when only a small portion of the background component is intercepted.

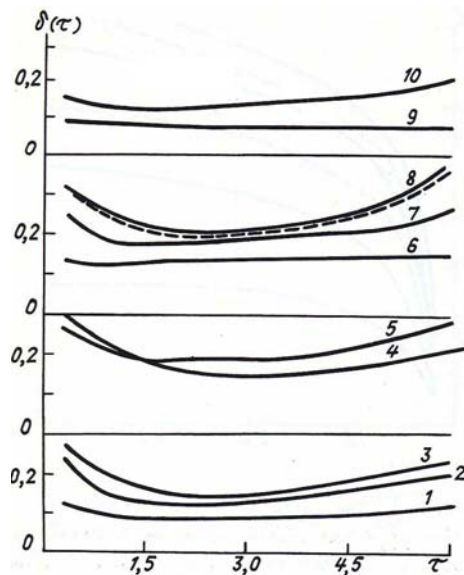


Fig. 2. Degree of depolarization $\delta(\tau)$ as a function of the parameter η , scattering phase function and probability of quantum survival W . $\sigma_{\text{ext}} = 0.33 \text{ m}^{-1}$; $W = 0.835$ everywhere except for curves 9 and 10 where $W = 0.63$; curves 1 to 4 were calculated using $g_2(9)$ scattering phase function, curves 5 to 10 using $g_1(9)$; the value of η is 0.02 for curves 1, 6, 9, $\eta = 0.06$ for curves 2, 7, 10, and $\eta = 0.12$ for curves 3, 4, 5, 8.

Curves 1–4 and 5–8 were calculated using scattering phase functions $g_2(9)$ and $g_1(9)$, respectively. At values of $\eta \leq 0.02$ and for $\phi_r = \phi_s$, the depth behavior of $\delta(\tau)$ is neutral function down to significant depths. If the medium being probed contains nonspherical particles, the degree of lidar depolarization is mainly determined by depolarization of the single scattering component of the return signal. The greater the degree of depolarization, of the singly-scattered component, the smaller its distortions due to multiple-scattering depolarization. Depolarization of the singly-scattered return by hydrosol particles is only moderate, and varies between 0.12 and 0.15. The stability of the behavior of $\delta(\tau)$ in sea water can be explained by the low depolarization of the background component of the lidar return $I_{\text{ph}}(r)$. This is due to the fact that because of the high asymmetry of the scattering phase functions (see Fig. 2, curves 4 and 5), secondary scattering takes place only in a narrow angular region around the direction of sounding beam propagation. Furthermore, for low values of $\eta \leq 0.02$ the contribution of molecular scattering to facilitating the preservation of the original signal polarization.

The calculations made using scattering matrices measured in model media^{7,8} (bacteria, diatomic algae, etc.) and in the Baltic Sea⁹ have shown that $\delta(\tau)$ varies within the same limits.

The absorbing component of sea water is highly variable. The absorption coefficient of clear water is practically the same in different waters, so variations in sea water absorption are mainly due to variations in phytoplankton and yellow matter concentrations (C_{ch} and C_{ym}). In the calculations, absorption of light is taken into account through the photon survival probability W .

The foregoing estimates (Fig. 2, curves 1 to 8) were made for waters of moderate productivity, where the value $W = 0.835$ for $C_{\text{ch}} = 0.2 \text{ mg/m}^3$ and $C_{\text{ym}} = 1$, values taken from Refs. 12, 13. The effects due to absorption are more pronounced in high productivity waters. Curves 9 and 10 in Fig. 2 were calculated for waters with high concentrations of absorbing components ($C_{\text{ch}} = 2 \text{ mg/m}^3$, $C_{\text{ym}} = 2$, $W = 0.63$). High absorption reduces the order of multiply scattered components of the background signal, which in turn reduces the depolarization $\delta(\tau)$ of the total lidar return signal (compare curves 9 and 10 with 6 and 7 in Fig. 2). It should be noted that low values of the photon survival probability can also occur in low-productivity waters of high transparency, since in that event the relative contribution of molecular absorption increases.

There can thus occur a situation in lidar sensing of such waters when the state of lidar return polarization is almost the same as that of sounding beam. In this regard, it is also worth recalling that increasing the contribution from molecular scat-

tering, in this case, also tends to decrease the degree of lidar return depolarization.

Calculations with the values of $C_{ch} = 0.1 \text{ mg/m}^3$, and $C_{ym} = 0.3$ (i.e., $W = 0.72$) have shown that in this case the degree of depolarization of lidar returns δ was about 0.12 to 0.15 at optical depths $\tau < 0.6$ and with the receiver's field of view φ_r being equal to $3\varphi_s$ (where φ_s is the sounding beam divergence).

As a matter of fact, minor fluctuations in C_{ch} and C_{ym} will not produce any marked changes in the lidar return polarization structure (see dashed curve in Fig. 1 for $W = 0.81$). The estimates of $\delta(\tau)$ for a "humid" atmosphere are given in Fig. 3. The calculations were made using the $g_1(9)$ scattering phase function. We observed the stable behavior of $\delta(\tau)$ noted above for $\eta \leq 0.02$, and increasing $\delta(\tau)$ with depth for $\eta > 0.02$. The atmospheric ground layer has no observable effect on the depth behaviour of $\delta(\tau)$.

Comparing the data in Fig. 3 with curves 6 to 8 in Fig. 2 we see that in a "humid" atmosphere, the influence of sounding beam depolarization in the atmosphere on the depth behaviour of $\delta(\tau)$ in water is noticeable only at depths of about 4 to 6 m below the air-water interface.

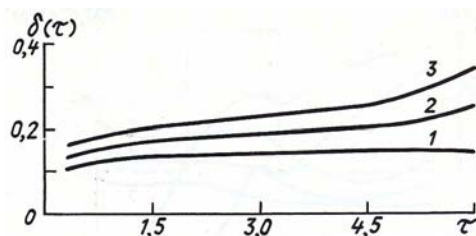


Fig. 3. Degree of depolarization in 'humid' atmosphere as a function of the parameter η at $\sigma_{ext} = 0.33 \text{ m}^{-1}$, and $W = 0.835$. The value of η is 0.02, 0.06 and 0.12 for curves 1, 2 and 3, respectively.

It is known that the optical characteristics of sea water do not remain the same at different depths. Without dwelling on the many physical processes responsible, note at the same time that the vertical distribution of $\sigma_{ext}(h)$ for different regions of the World's Oceans has its own fairly stable inherent characteristics¹⁵. This is normally related to hydrodynamic processes which determine the optical properties of water in each region.

The type of $\sigma_{ext}(h)$ profile is often determined by the depth at which the seasonal pycnocline (the layer of a sharp jump in water density) occurs. If it is deep-seated ($h \geq 50 \text{ m}$) or if intense turbulent mixing of water takes place, the optical properties of the surface layer will be relatively stable. The above assessments were made for such an optical situation. If the pycnocline is near the surface then one has a profile $\sigma_{ext}(h)$ that increases with depth in the upper layer of water, while the opposite behaviour of $\sigma_{ext}(h)$ occurs much more realy¹⁵. In ad-

dition, stratified layers of high optical depth can appear at some distance from surface of the water, due to various hydrodynamic, biological and other processes. It is interesting in this connection to assess the possible effects of different optical situations on the polarization characteristics of lidar returns. The estimates for "dry" atmosphere are presented in Fig. 4, where the histogram shows the model profiles for the extinction coefficient. For each of the profiles, the figure shows three curves $\sigma_{ext}(h)$ calculated for different angular apertures of the receiver. One can see in this figure that at small angular apertures $\varphi_r \leq \varphi_s$, the profile $\delta(h)$ is largely insensitive to changes in the optical structure of the water. This can be easily explained by recalling that the receiver field of view intercepts, in this case, radiation that has not been multiply scattered to any great extent, whose depolarization only slightly exceeds that of the singly-scattered signal. As the receiving angle increases, the return signal incorporates a greater contribution of light scattered at larger angles, which has higher depolarization, and as a result, the behaviour of $\delta(h)$ becomes more dependent on the shape of $\sigma_{ext}(h)$ profile.

The maximum receiving angle for which the calculations presented in Fig. 3 were made was if $\varphi_r = 2^\circ$. Further increases in this angle result in the background component exerting a decisive influence on the return signal. As a consequence, the degree of depolarization of the total signal becomes uniformly high over the whole range and the dependence of depolarization on $\sigma_{ext}(h)$ disappears. Note that in none of the examples considered did the value of $\delta(h)$ at the far end of the sounding path (at $\tau \sim 7$ to 8) exceed 0.5. Figure 4 also presents the profiles of lidar return signals $I(h)$. $I(h)$ shows a clear-cut dependence on the profile $\sigma_{ext}(h)$ only in the case of a stratified hydrosol inversion. In the other situations, a change in shape of $I(h)$ is accompanied by a change in $gradI(h)$.

Thus, only simultaneous analysis of $gradI(h)$ and $grad\delta(h)$ at a range of angular apertures of the receiver can provide qualitative information about the $\sigma_{ext}(h)$ profile.

In conclusion, it can be said that the numerical estimates presented above do not cover all the possible variety of optical properties of sea water. First of all, this relates to types of scattering matrices. In this paper, we used only the type which occurred in the majority of experimental studies, and which is close in general form to the Rayleigh type.

The estimations discussed in this paper have also shown that the type of sea water scattering phase function is an important factor in determining the polarization structure of the lidar return from the water. Lidar return depolarization can increase due to a decrease in the scattering phase function asymmetry, as well as an enhancement of backscatter caused by changes in hydrosol microstructure or fractional composition. At the same time our estimates have shown that 10 to 15 percent variations of scattering matrix elements observed experimentally by different authors⁶⁻⁹ do not result in any noticeable change in the polarization structure of lidar returns.

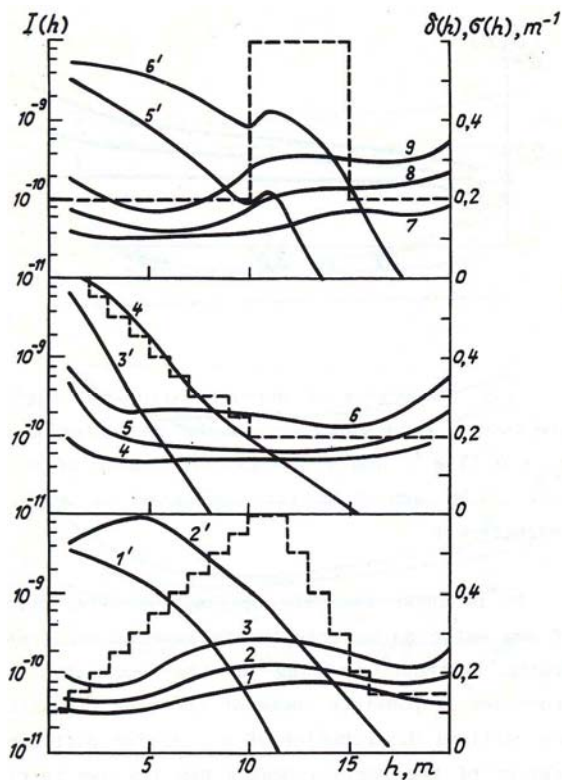


Fig. 4. Dependence of lidar return intensity $I(h)$ and its degree of depolarization on the profile $\sigma_{\text{ext}}(h)$, as calculated using the $g_1(9)$ scattering phase function. Curves 1' to 6' are $I(h)$; curves 1 to 9 are $\delta(h)$; $\eta = 0.02$ for curves 1, 4, 7 and 1'; 3'; 5'; $\eta = 0.06$ for curves 2, 5, 8 and 2'; 4'; 6'; $\eta = 0.12$ for curves 3, 6, 9; dashed lines show $\sigma_{\text{ext}}(h)$.

REFERENCES

1. V.E. Zuev, G.M. Krekov, G.G. Matvienko and A.I. Popkov in: Laser Sensing of the Atmosphere (Nauka, Moscow, 1976)
2. V.E. Zuev, G.M. Krekov and M.M. Krekova Izvestia Akad. Nauk SSSR, ser. Fizika Atmosfery i Okeana, **9**, 595 (1988)
3. G.M. Krekov and R.F. Rakhimov Optical Models of Atmospheric Aerosol (Izdat. TF SO AN SSSR, Tomsk, 1986)
4. R.J. Perry, J. Hant and D.R. Huffman "Experimental determinations of Mueller scattering matrices for nonspherical particles, Appl. Optics, **17**, (1978)
5. V.V. Belov, G.M. Krekov and G.A. Titov in: Topics in Remote Sensing of the Atmosphere ed. by V.E. Zuev, (Izdat. TF SO AN SSSR, Tomsk, 1975)
6. K.J. Voss and E.S. Fry "Measurement of the Mueller matrix for ocean water" Appl. Optics, **23**, 4427 (1984)
7. Ju.S. Lyubovsteva, G.S. Moiseenko and I.N. Plokhina Izvestia Akad. Nauk SSSR, ser. Fizika Atmosfery i Okeana, **13**, 1097 (1977)
8. R.C. Thompson, J.R. Bottigor and E.S. Fry "Scattering matrix measurements of oceanic hydrosols" SPIE, Ocean Optics, **60**, 43 (1979)
9. E.A. Kadyshevich Izvestia Akad. Nauk SSSR, ser. Fizika Atmosfery i Okeana, **13**, 108 (1977)
10. E.A. Kadyshevich, Yu.S. Lyubovtseva and G.V. Rosenberg Izvestia Akad. Nauk SSSR, ser. Fizika Atmosfery i Okeana, **7**, 557, (1971)
11. E.A. Kadyshevich, Yu.S. Lyubovtseva and G.V. Rosenberg Izvestia Akad. Nauk SSSR, ser. Fiz., **12**, 186, (1976)
12. O.V. Kopelevich in: Ocean Optics, **1**, Physical Optics of the Ocean, (Nauka, Moscow, 1983)
13. Remote Sensing of Sea with Allowance for the Atmosphere, ed. by V.A. Urdenko and G. Zimmermann, (ISR Acad. Sci. GDR, 1985)
14. M.M. Krekova, I.E. Penner and I.V. Samokhvalov, in Proc.: IX All Union Symposium on Laser and Acoustic Sensing of the Atmosphere, (Izdat. TF SO AN SSSR, Tomsk, 1987)
15. V.I. Burenkov in: Ocean Optics, **2**, Applied Ocean Optics, (Nauka, Moscow, 1983)